2012 Intelligent Vehicles Symposium
Alcalá de Henares, Spain, June 3-7, 2012

Roll Angle Estimation for Motorcycles: Comparing Video and Inertial Sensor Approaches

Marc Schlipsing*, Jan Salmen*,
Benedikt Lattke◇, Kai Gerd Schröter◇, and Hermann Winner◇

Abstract— **Advanced Rider Assistance Systems (ARAS) for powered two-wheelers improve driving behaviour and safety. Further developments of intelligent vehicles will also include video-based systems, which are successfully deployed in cars. Porting such modules to motorcycles, the camera pose has to be taken into account, as e. g. large roll angles produce significant variations in the recorded images. Therefore, roll angle estimation is an important task for the development of various kinds of ARAS. This study introduces alternative approaches based on inertial measurement units (IMU) as well as video only. The latter learns orientation distributions of image gradients that code the current roll angle. Until now only preliminary results on synthetic data have been published. Here, an evaluation on real video data will be presented along with three valuable improvements and an extensive parameter optimisation using the Covariance Matrix Adaptation Evolution Strategy. For comparison of the very dissimilar approaches a test vehicle is equipped with IMU, camera and a highly accurate reference sensor. The results state high performance of about 2 degrees error for the improved vision method and, therefore proofs the proposed concept on real-world data. The IMU-based Kalman filter estimation performed on par. As a naive result averaging of both estimates already increased performance an elaborate fusion of the proposed methods is expected to yield further improvements.**

I. Introduction

Driver assistance systems increase safety and comfort and thus become more and more important also for powered two-wheelers (PTW). Anti-Lock and Combined Brake Systems (ABS / CBS) as well as Traction Control Systems (TCS) are the most common Advanced Rider Assistance Systems (ARAS) on modern PTW. These and other applications aim at the stability of the vehicle in order to improve driving behaviour and safety. In this context the estimation of the vehicle's orientation and particularly the roll angle, i.e. the angle between the road plane and the inclined vehicle, is an essential task. Algorithms based on an inertial measurement unit (IMU) estimate the orientation of a vehicle by combining multiple sensory inputs, i. e. roll rate, velocity, acceleration, and GPS information.

For current and future developments in driver assistance, video-based systems are very popular and promise to provide information needed for safe, comfortable, and economic driving. Many applications deployed in cars and trucks already make use of video sensors in order to realise, for instance, recognition of obstacles, lane keeping, or traffic sign classification. Almost all of those applications rely on a rather constant orientation of the camera, which applies to systems mounted on a car. Transferring camera-based assistance systems or at least their functional back-ends to motorcycles is desirable but gives again rise to the task of estimating the vehicle orientation. In comparison to a car-mounted camera the PTW's roll angle accounts for the most significant change in the recorded images.

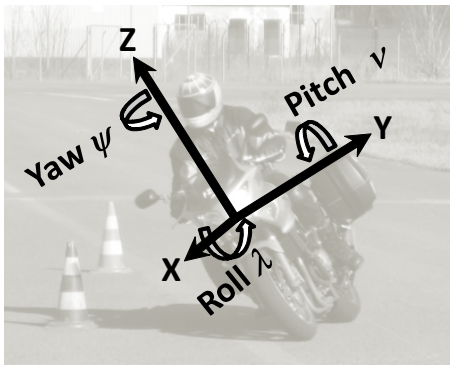

Fig. 1. Illustration of the motorcycle coordinate system.

Recently, Schlipsing et al. proposed a purely vision-based approach to roll angle estimation [1]. The novel method is based on learning orientation distributions of the image gradient that code the roll angle of the camera. Preliminary experiments were conducted on synthetically rolled images from a car-mounted camera and stated an error of about 2 degrees.

In this study, three alternative approaches are introduced and evaluated – two different IMU-based methods and an extension to [1], only relying on video images from a front-mounted camera. For the latter, three valuable enhancements are proposed and an evolutionary optimisation is applied to the essential parameters using the Covariance Matrix Adaptation Evolution Strategy (CMA-ES). The evaluation is done on real data, recorded from the same test vehicle, which at the same time collects ground truth data from a highly accurate IMU (i. e. ADMA-sensor) as a reference.

There are approaches to estimate vehicle states by integration of several sensor responses, i. e. velocity, acceleration, roll / pitch / yaw rate, and distance to ground plane [2][3][4][5][6]. Their setups include IMUs or other contact-free measurements in order to analyse vehicle dynamics or rely on visual information [7][8][9].

*Institut für Neuroinformatik, Ruhr-Universität Bochum, 44780 Bochum, Germany.
{marc.schlipsing,jan.salmen}@ini.rub.de
◇Fachgebiet Fahrzeugtechnik, Technische Universität Darmstadt, 64287 Darmstadt, Germany.
{lattke,schroeter,winner}@fzd.tu-darmstadt.de

The upcoming section briefly recalls the video-based method and points out its limitations, proposed extensions, and the applied evolutionary optimisation strategy. Section III presents two novel approaches to IMU-based roll-angle estimation. The experimental setup including the description of used sensors, the driving site and the applied test procedure will be given in Sec. IV. Experimental results in Sec. V will briefly compare the performance of the methods based on independent sensors and evaluate the performance gained from the extension and optimisation of the video-based approach. In the final Sec. VI findings are summarised and conclusions concerning the problem of roll angle estimation for motorcycles are drawn.

II. Video-based roll angle estimation

Typical road scenes feature recurring geometry and compositions of objects. Recording those scenes, characteristic orientation distributions can be found and learnt from image gradients that code the roll angle of the motorcycle. By correlating the statistics (orientation histogram) of a single image with the learnt counterpart, the displacement can be derived. This novel approach was introduced in [1]. The main motivation was a cost-efficient porting of video-based assistance modules originally developed for cars to motorcycles. Preliminary results showed great promise for a robust estimation from video only.

A. Original method

The learning algorithm is divided into training and test phase. Each processed image is represented by its gradient orientation distribution. It is therefor transformed to a low-dimensional angle histogram, capturing the occurrence frequency of reasonable angle intervals (see Fig. 2). In order to favour meaningful gradients, each orientation entry is weighted by its energy.

During training, which is performed offline, the orientation of the gradients are shifted by the corresponding roll angle (ground truth) towards a horizontal alignment. Thus, a mean histogram, coding the orientation distribution with respect to the horizon, can be derived over time.

During the test phase one is able to correlate each image's histogram with the learnt one. Therefor it is translated by a range of reasonable roll angles, i. e. $[-40°, 40°]$. The straight forward solution is to pick the translation with the maximum normalised cross-correlation (NCC) and perform quadratic interpolation within the direct neighbourhood.

Similarly, the roll rate is estimated. However, instead of the comparison with the learnt histogram, the correlation with one of the preceding images is maximised. Given the recording frequency of the camera, the measured roll angle can be derived in degree per second. Finally, both values are fed into a linear Kalman filter which is able to produce a smooth estimate of the roll angle, considering the physical relationship between the observed measures. For a detailed description and relevant formulas please refer to [1].

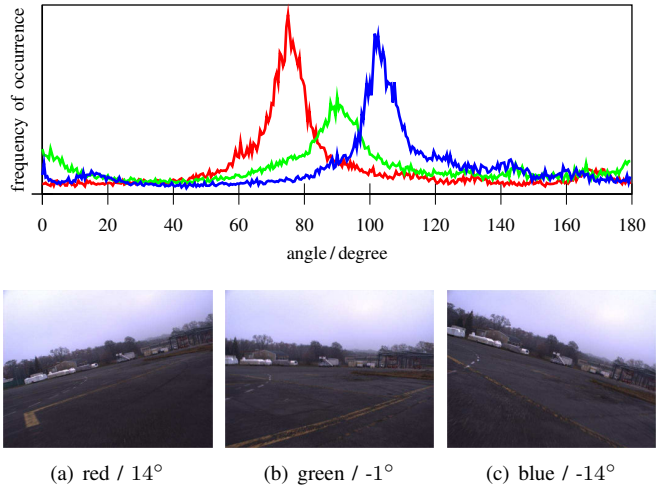

(a) red / 14° (b) green / -1° (c) blue / -14°

Fig. 2. Normalised orientation histograms of three closely recorded images and their corresponding ground truth roll angle.

B. Limitations

Due to the following considerations, it was unclear, to what extent the method would also perform well on real-world data: Evaluation was conducted on data from a car-mounted camera – simulating the rolling behaviour by simple image rotations, which is not sufficient to model the recording under a specific roll angle. Given various angles, the camera will record different parts of the scene in different perspectives. Moreover, the driving behaviour was modelled by a sine-wave, which is not sufficiently realistic. Vibrations and pitch angles due to accelerations are more intense on a motorcycle than in a car.

Thus, the approach was now evaluated on a two-wheeled test vehicle in order to quantify the error on realistic data and propose valuable extensions to the base algorithm.

C. Extensions

In some situations the main gradient orientations can be disturbed by strong local gradients, e. g. introduced by special lane markings or patterns. Those situations can often lead to very incorrect measurements, still featuring a high correlation coefficient. In order to increase robustness, the roll angle search algorithm was therefore extended by introducing a priority interval around the current estimate. The size of that range is introduced as an additional parameter for optimisation. As a side-effect, processing time decreases significantly.

The Kalman filter used to integrate and stabilise the individual estimates of angle and rate was originally initialised with physically reasonable and constant covariances for state noise and observation noises. The optimisation of those parameters is discussed in the following subsection. Moreover, the behaviour of the filter is enhanced by dynamically adjusting the noise covariances depending on the normalised cross-correlation coefficient of each measurement. For translating NCC measures c to noise (standard deviation σ)

$$\sigma = f(c) : [-1, 1] \rightarrow (0, \sigma_{\max}] \tag{1}$$

an inverse linear mapping starting at an NCC threshold $c_{\min}$ is proposed.

$$f(c) = \begin{cases} \frac{\sigma_{\max}}{c_{\min}-1}(c - c_{\min}) + \sigma_{\max} \ , c > c_{\min} \\ \sigma_{\max} \ , \text{otherwise} \end{cases} \quad (2)$$

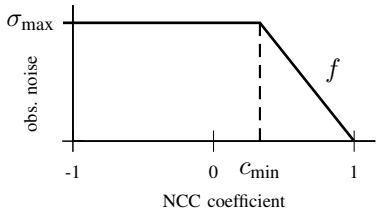

Fig. 3. Linear mapping of correlation measure to the Kalman filter's observation noise.

As negative correlation should never be regarded as a good match, $c_{\min} > 0$ is a reasonable limitation (see Fig. 3).

A third enhancement is proposed in order to filter the correlation results. Due to the discretisation introduced through the fixed histogram resolution (i. e. degree per histogram bin), artefacts are likely to emerge when correlating two histograms. Therefore, a one-dimensional binomial filter is applied to the correlation array during angle and rate estimation.

D. Parameter optimisation

During training and testing the described algorithm requires the choice of parameters. Some parameters result from the experimental setup (cf. Sec. IV), e. g. the maximum possible roll angle and rate. The following settings were optimised in order to approximate the optimal configuration.

Roll rate lookback: The number of frames between the current and the past image, that are used to estimate the roll rate. For the sake of real-valued optimisation the estimates of the two closest integer values are interpolated linearly.

Angle search range: The radius of the search interval around the current estimate (cf. Sec. II-C).

Observation noises: Maximal noise of the observations used for Kalman filtering (given in standard deviations). The observation noises are tuned with respect to a constant state noise of 1.

NCC thresholds: Minimal correlation of a measurement for which the observation noise is decreased (for both angle and rate individually).

The optimisation goal is the minimisation of the root mean squared error (RMSE) of the angle estimate over a sequence of images. As the gradient of the fitness function cannot be computed, direct search is performed in a real-valued parameter space.

Covariance Matrix Adaption evolution strategy (CMA-ES) [10] is a variable-metric evolutionary algorithm which represents the "state-of-the-art in evolutionary optimisation in real-valued search spaces" [11]. Several runs were conducted in parallel, each with a random starting point, observing the median RMSE until convergence. Results of the parameter evolution will be presented in Sec. V.

III. IMU-based Roll Angle Estimation

After stating the involved driving dynamics, this section introduces the two approaches based on inertial sensors.

A. Motorcycle Driving Dynamics

One way to calculate the roll angle λ is the integration of the roll rate $\dot{\lambda}$. This is described by the following equation:

$$\lambda = \int \dot{\lambda} \, \mathrm{d}t \quad (3)$$

According to Weidele [2], the tangent of the physical roll angle λ_{ph} is equal to the ratio of lateral force and gravitational force (for steady-state rides). This yields the following relation, depending on lateral acceleration a_{Y} and gravity acceleration g:

$$\tan \lambda_{\mathrm{ph}} = \frac{F_{\mathrm{S}}}{F_{\mathrm{G}}} = \frac{a_{\mathrm{Y}}}{g} \quad (4)$$

The lateral acceleration a_{Y} depends on the longitudinal vehicle velocity v_{X} and the horizontal yaw rate $\dot{\psi}$ as following (neglecting a side slip rate of the motorcycle):

$$a_{\mathrm{Y}} = -v_{\mathrm{X}} \cdot \dot{\psi} \quad (5)$$

Inserting equation (5) into (4) and transforming the horizontal yaw rate $\dot{\psi}$ into the measured body yaw rate $\dot{\psi}_{\mathrm{V}}$ results:

$$\tan \lambda_{\mathrm{ph}} = -\frac{v_{\mathrm{X}} \cdot \dot{\psi}_{\mathrm{V}}}{g \cdot \cos \lambda} \quad (6)$$

With the assumption $\lambda_{\mathrm{ph}} = 0.9 \cdot \lambda$, equation (6) delivers the following relation between roll angle λ, longitudinal vehicle velocity v_{X} and body yaw rate $\dot{\psi}_{\mathrm{V}}$:

$$\tan (0.9 \cdot \lambda) \cdot \cos \lambda = -\frac{v_{\mathrm{X}} \cdot \dot{\psi}_{\mathrm{V}}}{g} \quad (7)$$

B. Combined Filter Method

In a former study, Seiniger et al. [3] developed a method for calculating the roll angle that combines information from multiple vehicle dynamics sensors. In this paper, a simplified version of this method is used, employing the equations (3) and (7).

A roll angle calculation based on equation (7) is valid during steady-state riding. During dynamic manoeuvres, a calculation by using equation (3) yields good results. In other situations, integration errors are not negligible. A combination by using a low pass and a high pass filter (see Fig. 4) exploits the advantages of both calculation methods.

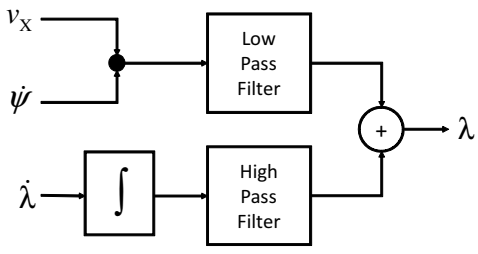

Fig. 4. Basic Principle of Combined Filter Method

C. Kalman Filter Method

A new approach employs the same equations (3) and (7) as the presented Combined Filter Method. However, instead of a combination of low and high pass filters, an Extended Kalman Filter with the following state vector is used:

$$\mathbf{x} = \left[v_{\mathrm{X}}, a_{\mathrm{X}}, \lambda, \dot{\lambda} \right]^T \tag{8}$$

Equation (3) is implemented by using a Constant Turn Rate Model for describing the roll motion. Equation (7) is implemented by introducing the "artificial" measurement $y_{\dot{\psi}_\mathrm{V}}$:

$$y_{\dot{\psi}_\mathrm{V}} = v_{\mathrm{X}} \cdot \dot{\psi}_{\mathrm{V}} = -\tan\left(0.9 \cdot \lambda\right) \cdot \cos\lambda \cdot g \tag{9}$$

With respect to the measurement of longitudinal vehicle velocity v_{X} and the roll rate $\dot{\lambda}$, this yields the following measurement model:

$$\mathbf{y} = \begin{pmatrix} \dot{\lambda} \\ y_{\dot{\psi}_\mathrm{V}} \\ v_{\mathrm{X}} \end{pmatrix} = \begin{pmatrix} \dot{\lambda} \\ -\tan\left(0.9 \cdot \lambda\right) \cdot \cos\lambda \cdot g \\ v_{\mathrm{X}} \end{pmatrix} \tag{10}$$

IV. Experimental Setup

This section will explain the sensory setup of the test vehicle, introduce the driving environment and point out the conditions of the conducted experimental session.

A. Motorcycle Sensors, Video and Data Acquisition

The on-board measurement setup, illustrated in Fig. 5, comprises two standard wheel speed sensors, a MEMS-based low-cost IMU mounted closely to the vehicle Center of Gravity (CoG) below the rider's seat, and a GPS-supported high-precision IMU (Genesys ADMA-G) in the left side-case for reference measurements of ground truth data. The measured signals are transferred with individually optimised sampling rates via a CAN-Bus-System. A modified Car-PC in the right side-case is running carhs viilab® software, serving for data-acquisition and control of the test vehicle's HMI.

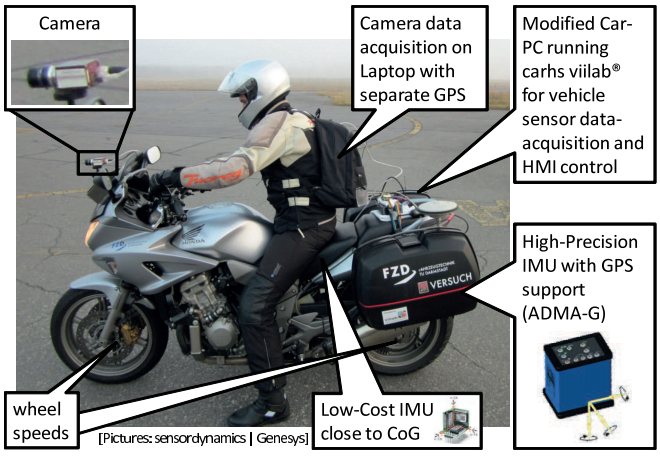

Fig. 5. Setup of test motorcycle

Fig. 6. Satellite image of the test site (source: *Google Maps*)

The video recordings were acquired independent from the on-board hardware. The used CCD-camera is a *Prosilica GC1380CH* with a resolution of 1.3 Mpixels and a Gigabit ethernet interface. It was mounted on the vehicle in front of the wind-shield, facing ahead. Data was recorded with a frame rate of 30 images per second on a standard laptop placed in the backpack of the rider. For later synchronisation with ground truth data an additional GPS signal was recorded.

B. Test Environment and Manoeuvres

Test drives were conducted on TU Darmstadt's proving ground, Griesheim Airfield, in foggy cold conditions. While diffused light is helpful for a good scene contrast, water drops on the lens blur the view. The test site offers a large runway, a taxiway, a turning circle and the area in front of the control tower with several buildings nearby (cf. Fig. 6). The asphalt surface partly features straight and circular lane markings like they can be found on urban streets or motorways. Nevertheless, in comparison to the acquisition of video data in real traffic scenarios the test site has a limited diversity.

The cold and partially wet road surface did not allow extreme driving manoeuvres. However, a set of generic manoeuvres with roll angles of up to 40° was performed, in order to simulate real driving on rural roads. Among others, these are straight driving, constant and variable radius cornering, swerving, and slalom. All manoeuvres were conducted in steady state or superimposed with acceleration or braking, which results in considerable pitch angles. Moreover, as the road-unevenness of the airfield is representative for rural roads, a realistic vertical excitation of the vehicle and video-picture can be assumed.

The goal of the experiments is an objective evaluation of the presented approaches to roll angle estimation and an analysis of their error characteristics. In particular, with these first experiments on real data, the feasibility of the novel image processing method is assessed in practice.

V. Results

Experiments were conducted on five sequences – two for training and optimisation of the camera-based methods and three for evaluation (I – III). This section features a brief comparison of the presented approaches, followed by a detailed optimisation analysis of the vision methods.

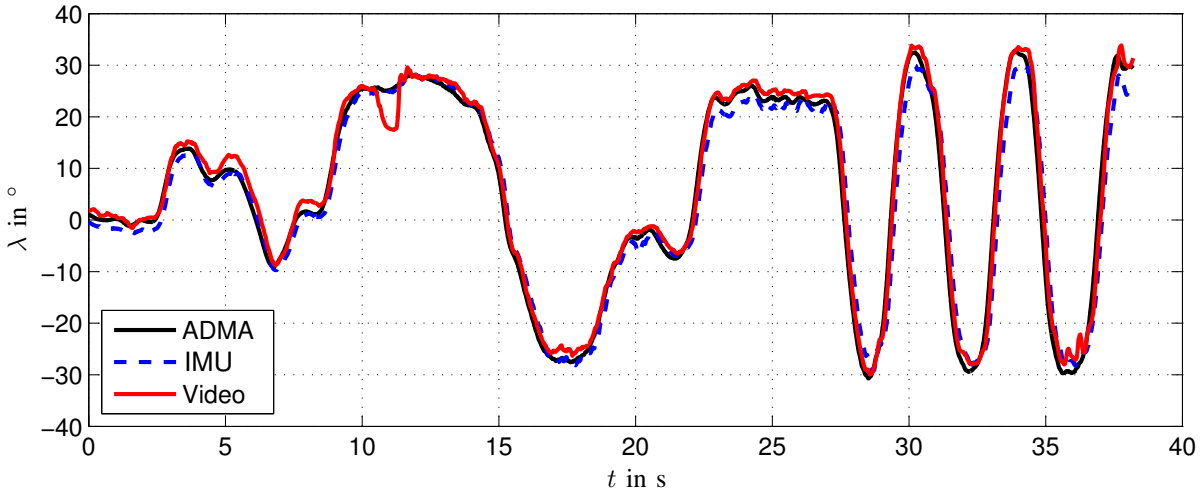

Fig. 7. Reference values (ADMA) and estimates of the roll angle for the IMU-based Kalman filter method (IMU) and the Video-based method (Video)

A. Comparison

Figure 7 shows the determined values of the roll angle for an excerpt of sequence III. Table I contains the root mean squared errors (RMSE) for all approaches and sequences. Among the IMU-based approaches, the Kalman filter method shows superior performance for the analysed test set. The proposed extended image processing approach reaches a similar performance level and outperforms its original (cf. Sec. V-B).

TABLE I
RESULTS (RMSE) FOR THREE DATASET GIVEN IN DEGREE.

method / sequence	I	II	III
Vision – original	3.57	5.48	3.60
Vision – new	2.24	2.78	2.26
IMU – Combined filter	3.75	4.06	3.73
IMU – Kalman filter	2.01	2.23	2.04
Mean Vision/IMU	1.20	1.37	1.68

With regard to the ADMA reference, the Kalman filter method and the video-based method show their largest deviations at different times. As indicated by the last row of Tab. I, already a naive averaging of the independent estimates causes a significant decrease in error. Therefore, a more elaborate combination of the two methods, taking detailed error analysis into account, is expected to yield further improvements.

B. Analysis of video-based method

One of the training sequences was used to learn the statistics of the given camera setup, the other for minimising the error through CMA-ES for both original and extended (new) method. For computational efficiency of the search, several fixed angle histogram resolutions were chosen between $1/4°$ and $4°$. Figure 8 depicts the learnt histogram for a resolution of $1/2°$.

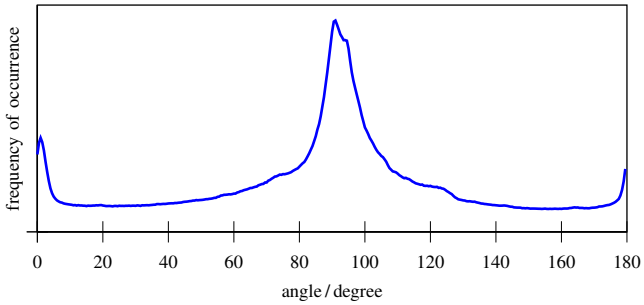

Fig. 8. Normalised histogram of the learnt gradient angles (resolution $1/2°$) from the training sequence.

Evolution starting points were chosen randomly within reasonable parameter intervals. In order to increase the probability of finding the globally optimal solution, nine evolution runs were conducted in parallel for each experiment. Figure 9 shows the median RMSE over the number of iteration. The final training error for both methods is stated numerically in Tab. II.

Two conclusions can be drawn from those evidences. Firstly, the novel approach yields significantly lower error on the training sequence and, secondly, the histogram resolution does not influence the performance much. In particular, a resolution finer than 1/2° does not pay off – especially taking the increasing computational complexity into account.

In order to assess the generalisation behaviour, both meth-

TABLE II
RESULTS (RMSE) OF ORIGINAL AND PROPOSED METHOD FOR EACH OF THE TESTED HISTOGRAM RESOLUTIONS (IN DEGREE) AFTER OPTIMISATION.

method	$\frac{1}{4}$	$\frac{1}{3}$	$\frac{1}{2}$	1	2	4
original	3.45	3.40	3.57	5.48	6.80	4.06
new	1.97	2.07	2.03	2.09	2.15	2.61

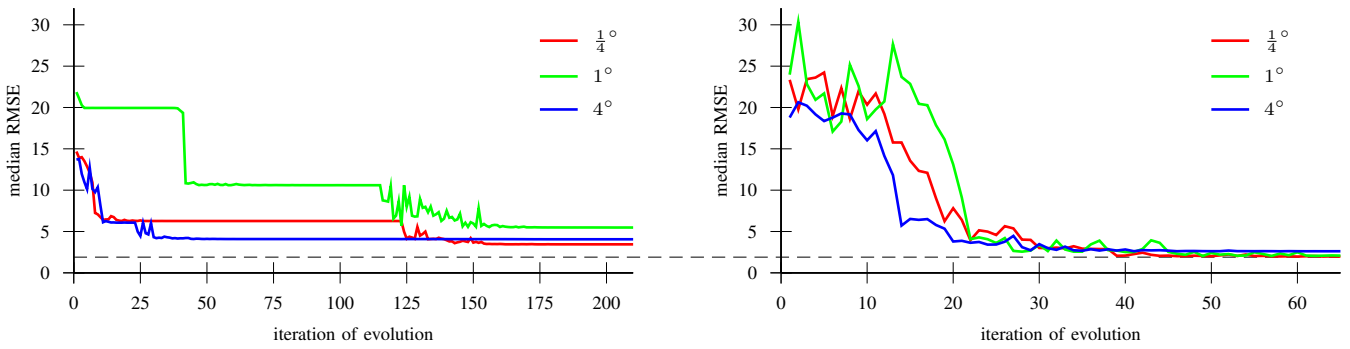

(a) Original method (3 parameters).

(b) Proposed method (6 parameters).

Fig. 9. Results of the CMA-ES optimisation for selected histogram resolutions ($0.25° - 4°$). While several thousands of iterations were performed, the plots limits to the most relevant excerpts until convergence.

ods were evaluated on the three test sequences with the best parameter set, documented in Tab. III. The optimal interval for estimating the roll rate translates to 170 ms and 265 ms, respectively. The choice of the newly introduced offsets for an observation noise adaption based on the NCC shows that a measurement with correlation below 0.7 for the angle and 0.9 for the rate is not trusted. The search interval of $12.7°$ speeds up the angle estimation by a factor of 3. Optimising the computational complexity was not a goal and might easily reduce the interval size without loss of accuracy.

TABLE III

OPTIMAL PARAMETERS FOR BOTH ORIGINAL AND EXTENDED VISION-BASED METHOD (CF. SEC. II-D).

parameter / method	original	new
lookback / frames	5.07	7.94
obs. noise $\sigma_{\max}(\alpha)$	0.145	0.0117
obs. noise $\sigma_{\max}(\alpha')$	0.0676	0.0933
NCC offset $c_{\min}(\alpha)$	–	0.669
NCC offset $c_{\min}(\alpha')$	–	0.906
search radius / °	–	12.7

Going back to Tab. I it can be concluded that the original approach of video-based roll angle estimation performed clearly worse compared to the evaluation on the synthetic data [1]. The extensions made to the algorithm, were able to significantly improve performance on real data.

VI. CONCLUSION

For the development of different ARAS, roll angle estimation plays an important role. This study presented two alternative IMU-based estimators featuring different filters. Moreover, extensions to a recently published method of roll angle estimation based on video images only were proposed and system parameters have been optimised using CMA-ES.

For an unbiased comparison, a common driving experiment was set up and conducted. The corresponding evaluation yielded a robust estimation at a mean precision of about two degrees for the improved vision method and, therefore, proofs the proposed concept on real-world data. Among other improvements, mapping the involved correlation confidences to observation noises for the Kalman filter update increased performance significantly with respect to the original method.

With regard to the reference, the IMU-based Kalman filter method and the video-based method perform on par. It is noteworthy that both produce their largest errors in different situations and simple averaging of the two estimates increases performance. Thus, an elaborate result fusion of these two methods is expected to yield further improvements. Examining this in the context of everyday traffic environments is planned for future research.

REFERENCES

[1] M. Schlipsing, J. Schepanek, and J. Salmen, "Video-based roll angle estimation for two-wheeled vehicles," in *Proceedings of the IEEE Intelligent Vehicles Symposium*, 2011, pp. 876–881.

[2] A. Weidele, "Untersuchungen zum Bremsverhalten von Motorrädern unter besonderer Berücksichtigung der ABS-geregelten Kurvenbremsung," in *Fortschritt-Berichte VDI*, vol. 12, no. 210, 1994.

[3] P. Seiniger, H. Winner, K. Schröter, F. Kolb, A. Eckert, and O. Hoffmann, "Development of a roll angle sensor technology for future brake systems," in *Proceedings of the International Motorcycle Conference*, 2006, pp. 369–388.

[4] A. Rehm, "Estimation of vehicle roll angle," *International Symposium on Communications, Control and Signal Processing*, pp. 1–4, 2010.

[5] J. Ryu and J. C. Gerdes, "Estimation of vehicle roll and road bank angle," in *Proceedings of the American Control Conference*, vol. 3, 2004, pp. 2110–2115.

[6] I. Boniolo, M. Norgia, M. Tanelli, C. Svelto, and S. Savaresi, "Performance analysis of an optical distance sensor for roll angle estimation in sport motorcycles," in *Proceedings of the IFAC World Congress*, 2008, pp. 135–140.

[7] L. Gasbarro, A. Beghi, R. Frezza, F. Nori, and C. Spagnol, "Motorcycle trajectory reconstruction by integration of vision and mems accelerometers," in *Proceedings of the Conference on Decision and Control*, 2004, pp. 779–783.

[8] F. Nori and R. Frezza, "Accurate reconstruction of the path followed by a motorcycle from the on-board camera images," in *Proceedings of the IEEE Intelligent Vehicles Symposium*, 2003, pp. 259–264.

[9] R. Labayrade and D. Aubert, "A single framework for vehicle roll, pitch, yaw estimation and obstacles detection by stereovision," in *Proceedings of the IEEE Intelligent Vehicles Symposium*, 2003, pp. 31–36.

[10] N. Hansen and A. Ostermeier, "Completely derandomized self-adaptation in evolution strategies," *Evolutionary Computation*, vol. 9, no. 2, pp. 159–195, 2001.

[11] H.-G. Beyer, "Evolution strategies," *Scholarpedia*, vol. 2, no. 8, p. 1965, 2007.